

Multiple targets direction-of-arrival estimation in frequency scanning array antennas


ISSN 1751-8784

Received on 3rd February 2015

Accepted on 29th August 2015

doi: 10.1049/iet-rsn.2015.0401

www.ietdl.org

Mona Akbarniai Tehrani , Jean Jacques Laurin, Yvon Savaria

Department of Electrical Engineering, École Polytechnique de Montréal, Montréal, Canada

✉ E-mail: mona.akbarniai-tehrani@polymtl.ca

Abstract: In this study, the authors address the problem of resolving angular position of multiple targets in the same range and separated by less than an antenna beamwidth using frequency scanning array (FSA) antennas. First, the frequency scanning antenna signal model is derived and then the necessary compensation methods to overcome antenna pattern variations with frequency during the scan in FSAs are presented. Two direction-of-arrival (DOA) estimation algorithms, the minimum variance beamforming and the maximum-likelihood estimation are applied on the signal model. Simulation results show that both methods can separate targets with angular separations smaller than a beamwidth by selecting correct parameters. The performance of the two DOA estimation methods with respect to different system parameters are investigated based on the signal model through Monte Carlo simulations and compared with the Cramér–Rao lower bound. In addition, an FSA antenna is presented in this work and simulations of the DOA estimation algorithms are performed using the measured antenna pattern of this antenna. The performance and limitations of target DOA estimation methods for the measured antenna patterns are also discussed.

1 Introduction

Low-cost electronically scanning radars for commercial applications are receiving considerable attention. Frequency scanning arrays (FSAs) are a solution to achieve low-cost and agile electronically scanning radars, without the need for phase shifters on the array elements. Unlike conventional FSAs that require frequency variation over a wide bandwidth [1], new FSAs using dispersive feed networks based on metamaterial guiding structures, can scan a wide angular range using a small bandwidth [2]. Therefore, using FSAs become practical in term of frequency bandwidth allocation. However, when the length of the array is limited, the width of its main beam can be wider than needed for a typical radar application, which results in poor angular resolution. Thus the appropriate signal processing for improving the angular resolution is necessary.

Examples of FSA utilisation in high resolution radars are presented in [3, 4]. This paper is considering a system that is used to estimate the angular position of targets using standard direction of arrival (DOA) algorithms. A pulsed step frequency mode of operation is assumed. Although angular resolution in an FSA antenna is obtained along with range resolution in [5, 6], improving angular resolution beyond beamwidth limitations in FSA has not been studied. Consequently, considering the low cost of FSAs compared to phased arrays, it is relevant to develop methods to improve the angular resolution of systems based on such antennas.

Unlike phased array antennas, in FSAs, all the radiating elements are fed with a waveguide having a frequency dispersive characteristic. So, the array elements can be assumed connected to each other and there is only one input/output port for all the antenna elements. Therefore the FSA can be modelled like a mechanically or electronically scanning antenna, with the difference that each part of the field of view (FOV) is illuminated by a different frequency related to the angle of transmission. This differs from multipoint antennas such as phased arrays in which elements can be weighted to shape the beam.

There are several superresolution algorithms that are able to detect signals separated by less than an antenna beamwidth. These algorithms are making use of multi-channel array antennas. DOA estimation methods based on maximum-likelihood (ML) [7] and

superresolution subspace methods like MUSIC [8] and ESPRIT [9] are some of the most well-known algorithms. However, there has been little work on improving angular resolution of a single channel antenna, so that it can resolve signals from directions separated by less than one beamwidth [11–15, 17–21]. In this work, we use two angular resolution improvement methods, minimum variance beamforming (MVB) [10] and ML estimation, which were previously applied to mechanically scanning antennas [11, 12] and adapt them for FSA antennas.

The paper is organised as follows. Section 2 briefly reviews the literature on single channel antenna superresolution and DOA estimation domain. In Section 3, a signal model that applies to FSA antennas is presented. In Section 4, the necessary compensation methods used to overcome gain and antenna pattern variations with frequency during the scan in FSA are presented. In Section 5, the MVB and ML estimation methods are briefly described. In Section 6, representative simulation results are given and the performance of selected methods with respect to different system parameters is evaluated. In Section 7, an FSA antenna is presented and the performance of the ML and MVB methods are evaluated for this FSA. Conclusions and remarks are provided in Section 8.

2 Brief overview of recent works on DOA estimation with single channel antennas

Most of the work in the single channel antenna superresolution and DOA estimation domains is based on the fact that antenna scanning induces amplitude modulation on signal backscatters and therefore, by utilising prior knowledge of the antenna pattern, the angular position of targets can be extracted [13, 14]. For example, Ly *et al.* [15] developed a MUSIC-based technique called scan-MUSIC (SMUSIC) to resolve target positions within a beam. In this method, the signal amplitude vector is formed using the response of the antenna as it scans the FOV. This differs from multi sensor array antennas in which multiple sensor outputs is used to form the signal amplitude vector. However, subspace-based methods do not work in the presence of correlated signals. To resolve correlated signals, in [15] the signal vector is divided into subvectors and a forward subvector averaging is

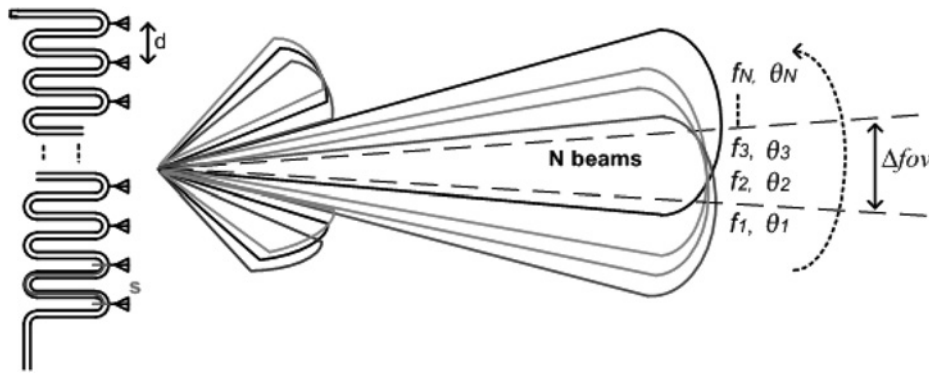


Fig. 1 Schematic representation of a frequency scanning antenna and the process of selecting N frequencies for which the main beam is in the Δfov angular range

performed as a form of spatial smoothing [16]. The author [17] proposed a technique based on interpolation of multiple shifted signal vectors from beamspace data to virtual multi sensor array antennas. Spatial smoothing is then applied to the interpolated vectors. This method has performance limitations due to nonuniform signal-to-noise ratio (SNR) profile across the interpolated vectors.

As an alternative to MUSIC-based methods, beamforming approaches can be applied to the signal amplitude vectors. Alvarez-Lopez *et al.* [5] studied the special case of a conventional beamformer in FSA antennas. Capon's MVB is also used in [17] to resolve DOA of signals in scanning antennas. Extension of the MVB method for step scanning radars is proposed in [11]. Unlike MUSIC-based methods, beamforming methods do not need prior knowledge on the number of targets. In [12], DOAs of multiple radar targets present in the main beam of a rotating antenna are estimated using the same concept as in [15] to form signal amplitude vector and by applying the ML technique. Both cases of conditional and unconditional ML are studied in [12]. A simplified version of the same method is presented in [18] as the pseudo-monopulse algorithm for target direction estimation and compared with the monopulse technique. An asymptotic ML estimator is also used in [19, 20] for detecting targets and estimating their complex amplitude and DOA in mechanically rotating antennas.

In [21], DOAs of multiple uncorrelated sources in single channel scanning antennas are estimated by measuring the power of the radiation pattern received during scanning. Then the vector of power measurements is transformed into a vector of spectral observations. Finally, DOA estimation is performed by spectral analysis methods.

In this paper, the effectiveness and performance of two of the above methods, MVB with spatial smoothing and ML estimation, when applied to FSA antennas are evaluated and compared. Using an FSA antenna, there is no need for mechanical rotation of the antenna which could be an advantage if targets move rapidly. FSA also enables agile operation not limited by constraints of mechanical systems. The selected methods are applicable to coherent signals and therefore they are able to estimate DOA of multiple targets.

3 Problem formulation

In FSA antennas, the main beam direction varies by changing the carrier frequency of the transceiver. This is achieved by using a series feed structure, in which the phase shift between adjacent element ports varies as a function of frequency. Using the simple delay line concept, the direction of the beam θ_m can be expressed as

$$\sin(\theta_m) = \frac{\lambda}{d} \left(\frac{s}{\lambda_g} - a \right) \quad (1)$$

where s is the length of the feed line between element ports, λ is the

free-space wavelength, λ_g is the wavelength in the feed line, d is the distance between radiating elements in the aperture plane, and a is an integer (see Fig. 1) [3]. The main beam direction θ_m is taken with respect to the normal of the antenna aperture. When the frequency varies, λ and λ_g change at different rates, which causes a variation of θ_m .

The FOV of the antenna corresponds to the angular sector scanned by the main beam direction when the frequency is swept over the complete frequency bandwidth of the antenna. Consider K targets present in the FOV at the same known range of $R_t = ct_l/2$, where t_l is the time for receiving an echo from targets at the range R_t and c is the speed of light. When the antenna main beam of an FSA radar is steered in the direction θ_m , the received baseband signal can be written as

$$x_r(t_l, \theta_m) = \sum_{k=1}^K s_k(f_m) g_m(\gamma_k) e^{-j2\pi f_m t_l} + n(t_l, \theta_m), \quad (2)$$

where f_m is the carrier frequency when the FSA beam is pointed at the angle θ_m , $s_k(f_m)$ is the complex signal scattered from the k th target with the angular position γ_k , $g_m(\gamma_k)$ is the two-way antenna pattern at the angle γ_k when the antenna is pointed at the angle θ_m (see Fig. 2), and $n(t_l, \theta_m)$ is the complex white Gaussian noise coming from the scene and introduced by the receiver components. It has been assumed that the Doppler shift of the echo can be neglected.

If the antenna pattern is approximated with a virtual linear array antenna pattern as

$$h(\theta_m, \gamma_k) = H_m \frac{\sin(N_e \psi/2)}{\sin(\psi/2)}, \quad \psi = \beta d [\sin(\gamma_k) - \sin(\theta_m)], \quad (3)$$

where H_m is the maximum gain, N_e is the number of elements in the array antenna, and β is the wave number, the two-way antenna pattern at the angle γ_k when the antenna is pointed at the angle θ_m can be approximated as

$$g_m(\gamma_k) = h^2(\theta_m, \gamma_k). \quad (4)$$

It is assumed that the phase response of the antenna pattern can be removed by appropriate a priori calibration of the FSA. In the vector notation of the signal model, the complex echo signal vector and the steering vector for a target at angle γ_k , when the antenna is steered to the angles θ_m with $m = 1, \dots, M$ are defined as

$$\mathbf{s}_k = [s_k(f_1), s_k(f_2), \dots, s_k(f_M)]^T, \quad (5)$$

$$\mathbf{a}(\gamma_k) = [a(\theta_1, \gamma_k), a(\theta_2, \gamma_k), \dots, a(\theta_M, \gamma_k)]^T, \quad (6)$$

where $(\cdot)^T$ denotes the transpose operation, M is the total number of

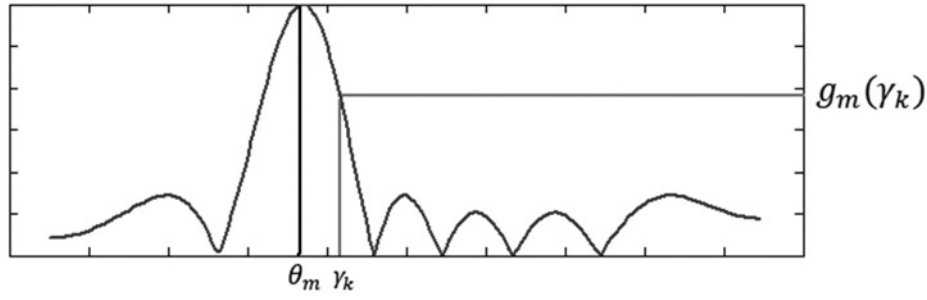


Fig. 2 Two-way antenna gain pattern

the frequencies, and steering vector elements are

$$a(\theta_m, \gamma_k) = g_m(\gamma_k) e^{-j2\pi f_m t_l}. \quad (7)$$

With K targets at directions $\gamma = [\gamma_1, \gamma_2, \dots, \gamma_K]$, the antenna response matrix and targets echo matrix are

$$A(\gamma) = [a(\gamma_1), a(\gamma_2), \dots, a(\gamma_K)], \quad (8)$$

$$S = [s_1, s_2, \dots, s_K]. \quad (9)$$

Equation (2) can be rewritten in the vector form as

$$\mathbf{x}_r = (A(\gamma) \odot S) \mathbf{I}_{K \times 1} + \mathbf{n} \quad (10)$$

where \odot is the Hadamard product $\mathbf{I}_{K \times 1}$ is a column vector of ones, and \mathbf{x} and \mathbf{n} are

$$\mathbf{n} = [n(t_l, \theta_1), n(t_l, \theta_2), \dots, n(t_l, \theta_M)]^T \quad (11)$$

$$\mathbf{x}_r = [x_r(t_l, \theta_1), x_r(t_l, \theta_2), \dots, x_r(t_l, \theta_M)]^T. \quad (12)$$

Note that the received signal $x_r(t_l, \theta_m)$ comprises the responses of all the visible targets when the FSA is operated at frequency f_m . It has been assumed that the targets cross sections do not change when the transmitted frequency changes, which may be a valid assumption when the used bandwidth is narrow. Then we have

$$s_k = s_k(f_1) = s_k(f_2) = \dots = s_k(f_M), \quad (13)$$

and

$$\mathbf{s} = [s_1, s_2, \dots, s_K]^T. \quad (14)$$

Thus the data model can be simplified to

$$\mathbf{x}_r = A(\gamma) \mathbf{s} + \mathbf{n}. \quad (15)$$

The objective is to estimate the vector of target angular positions γ while the targets complex echo vector, \mathbf{s} is unknown.

4 Calibration and interpolation

When using FSAs, some preprocessing steps are required before applying subspace-based target DOA estimation methods in which spatial smoothing is required. Spatial smoothing works when steering vectors can be divided into shift invariant overlapping subvectors [16]. It can be easily shown that shift invariant subvectors can be formed from the steering vector only if:

(i) the steering vector only includes the main beam of the antenna pattern,

(ii) the gain of the antenna pattern in different steering angles are balanced, and
 (iii) the angular separation between steering angles $(\theta_m - \theta_{m+1})$ are uniform.

In order to achieve the above properties the following compensation methods are considered.

First, the FOV is divided into several sectors called Δfov and DOA estimation methods are performed for each Δfov separately to find targets that are present in that sector. Using small Δfov reduces the computational complexity. In addition, for each Δfov , only N of the frequencies ($N < M$) for which the main beam belongs to that Δfov , are used in (5)–(14) (Fig. 1). As mentioned before, using our signal model, the subspace-based target DOA estimation methods work well only if, for each Δfov , only the beams having their main beam in that sector are considered in the superresolution computations.

Furthermore, in a practical FSA the maximum gain of the antenna pattern always varies with frequency. This variation must be compensated using suitable calibration prior to processing. To compensate existing gain imbalance, one of the N frequencies in the set of fixed frequencies f_n ($n = 1, \dots, N$) is selected as a reference (f_r), and the ratio between the amplitude of antenna pattern for the corresponding reference pointing angle (θ_r) with respect to other steering angles are chosen as compensation weights $c(\theta_n) = g_r(\theta_r)/g_n(\theta_n)$. The compensation matrix is then formed as follows:

$$\mathbf{c} = \text{diag}[c_1, c_2, \dots, c_N], \quad (16)$$

and the calibrated antenna response matrix $A_c(\gamma)$ is

$$A_c(\gamma) = \mathbf{c} A(\gamma). \quad (17)$$

Therefore, (15) can be modified to

$$\mathbf{c} \mathbf{x}_r = A_c(\gamma) \mathbf{s} + \mathbf{c} \mathbf{n}. \quad (18)$$

This process involves antenna pattern measurement and it has to be done once offline.

Moreover, according to (1), by changing the frequency in uniform steps, the antenna steering angle will change non-linearly. In other words, the steps between steering angles $[\theta_1, \theta_2, \dots, \theta_N]$ are not equal. We can thus write

$$\theta_n = \theta_1 + \sum_{i=1}^{n-1} \Delta\theta_i \quad (19)$$

where $\Delta\theta_i$ is the angular step between beam steering angles. While in some FSAs this non-linearity can be small and negligible, the performance of spatial smoothing degrades when uniform frequency steps are assumed in the model. Therefore, an interpolated version of $A_c(\gamma)$ can be used in (18) in which the relation between steering angle and frequency is linear.

Interpolation is performed using a method similar to the algorithm presented in [22] by computing an interpolation matrix.

First, for each sector (Δfov) a set of interpolation angles is defined

$$\Gamma = [\bar{\gamma}_1, \dots, \bar{\gamma}_D] \quad (20)$$

where D is the number of hypothetical DOAs of targets that are only used for interpolation.

Then, an interpolation matrix is computed by mapping $\mathbf{A}_c(\Gamma) = [\mathbf{a}_c(\bar{\gamma}_1), \mathbf{a}_c(\bar{\gamma}_2), \dots, \mathbf{a}_c(\bar{\gamma}_D)]$ to a virtual matrix $\bar{\mathbf{A}}(\Gamma) = [\bar{\mathbf{a}}(\bar{\gamma}_1), \bar{\mathbf{a}}(\bar{\gamma}_2), \dots, \bar{\mathbf{a}}(\bar{\gamma}_D)]$. This is done so that in each virtual steering vector $\bar{\mathbf{a}}(\bar{\gamma}_d) = [\bar{a}(\theta_1, \bar{\gamma}_d), \bar{a}(\theta_2, \bar{\gamma}_d), \dots, \bar{a}(\theta_N, \bar{\gamma}_d)]^T$ the steps between virtual steering angles $[\theta_1, \theta_2, \dots, \theta_N]$ will be equal:

$$\bar{\theta}_n = \theta_1 + (n-1)\Delta\theta, \quad \Delta\theta = \frac{|\theta_1 - \theta_N|}{N} \quad (21)$$

with $n = 1, \dots, N$. It is assumed that the virtual matrix $\bar{\mathbf{A}}(\Gamma)$ can be obtained by linear interpolation of the real matrix $\mathbf{A}_c(\Gamma)$, so that

$$\bar{\mathbf{A}}(\Gamma) = \mathbf{B}\mathbf{A}_c(\Gamma) \quad (22)$$

In which the interpolation matrix \mathbf{B} is the least square solution of (22) that should be found only once offline.

Thus, the signal model in (15) can be modified to

$$\bar{\mathbf{x}}_r = \mathbf{B}\mathbf{c}\mathbf{x}_r = \mathbf{B}\mathbf{c}\mathbf{A}(\boldsymbol{\gamma})\mathbf{s} + \mathbf{B}\mathbf{c}\mathbf{n}, \quad (23)$$

where $\bar{\mathbf{x}}_r$ is the corrected received data vector. Note that noise is no longer white in (23) and noise-whitening is also required.

5 DOA estimation methods

Brief descriptions of the target DOA estimation methods exploited in this paper are presented in this section for completeness.

5.1 Minimum variance beamforming

Using adaptive beamforming, a weight vector (\mathbf{w}) is applied to the corrected received data vector $\bar{\mathbf{x}}_r$ in a way that in the beamformer output the desired signals are emphasised and noise is suppressed

$$\mathbf{y} = \mathbf{w}^H \bar{\mathbf{x}}_r. \quad (24)$$

MVB is an adaptive beamforming approach which determines the optimum weight vector by minimising the power of signal plus noise at the output of an adaptive beamformer $E[|\mathbf{w}^H \bar{\mathbf{x}}_r|^2]$. The minimisation is subject to the constraint that the response of the beamformer to the desired signal with parameter $\boldsymbol{\gamma}$ is fixed [10]. The optimisation problem can be stated as

$$\min_{\mathbf{w}} \mathbf{w}^H \hat{\mathbf{R}} \mathbf{w} \quad \text{subject to} \quad \mathbf{w}^H \bar{\mathbf{a}}(\boldsymbol{\gamma}) = 1, \quad (25)$$

where $\bar{\mathbf{a}}(\boldsymbol{\gamma}) = \mathbf{B}\mathbf{a}(\boldsymbol{\gamma})$ and the sampled data covariance matrix $\hat{\mathbf{R}}$ is

$$\hat{\mathbf{R}} = \frac{1}{L} \sum_{l=1}^L \bar{\mathbf{x}}_r \bar{\mathbf{x}}_r^H, \quad (26)$$

L is the number of snapshots or complete scans over the FOV. The solution to the optimisation problem in (25) is

$$\hat{\mathbf{w}}(\boldsymbol{\gamma}) = \frac{\hat{\mathbf{R}}^{-1} \bar{\mathbf{a}}(\boldsymbol{\gamma})}{\bar{\mathbf{a}}^H(\boldsymbol{\gamma}) \hat{\mathbf{R}}^{-1} \bar{\mathbf{a}}(\boldsymbol{\gamma})} \quad (27)$$

and the estimate of output power at direction $\boldsymbol{\gamma}$ is

$$P_y(\boldsymbol{\gamma}) = \frac{1}{\bar{\mathbf{a}}^H(\boldsymbol{\gamma}) \hat{\mathbf{R}}^{-1} \bar{\mathbf{a}}(\boldsymbol{\gamma})} \quad (28)$$

If the target response is coherent, $\hat{\mathbf{R}}$ will be rank deficient and the algorithm will fail to resolve targets. To decorrelate target responses and to obtain a full rank covariance matrix, spatial smoothing [16] can be used. In spatial smoothing, the sampled data vector is divided into overlapping subvectors of $\bar{\mathbf{x}}_r^{(i)}$ for $1 < i < p$, where p is the number of subvectors each containing Q samples of $\bar{\mathbf{x}}_r$, so that $p = N - Q + 1$. The data covariance matrix can be then estimated by

$$\hat{\mathbf{R}}_f = \frac{1}{p} \sum_{i=1}^p \hat{\mathbf{R}}^{(i)} \quad (29)$$

Spatial smoothing works when the number of subvectors is equal to or larger than the number of targets ($p \geq K$) and the size of each subvector Q is at least $K + 1$ [16]. Therefore, we have

$$N \geq 2K. \quad (30)$$

The optimal subvector size is computed in [23] as

$$Q_{\text{opt}} = 0.6(N + 1). \quad (31)$$

5.2 ML estimation

The use of ML to estimate multiple target directions in scanning antennas is presented in [12]. The same method can be used for the case of an FSA antenna as the FSA signal model is similar to the one found in [12]. The only difference is that in the FSA signal model, the antenna response matrix $\mathbf{A}(\boldsymbol{\gamma})$ contains an extra phase term. Note that the interpolation step is not needed for the ML estimation method and the signal model in (18) or (15) is used for this method. Considering that each element of the noise vector \mathbf{n} has a white complex Gaussian probability distribution function with zero mean and variance of σ^2 , \mathbf{n} is modelled as white complex Gaussian noise with zero mean and covariance matrix of $\sigma^2 \mathbf{I}$

$$\mathbf{n} \sim \mathcal{CN}(0, \sigma^2 \mathbf{I}), \quad (32)$$

Therefore, the probability density function of the data vector \mathbf{x}_r conditioned to the unknowns ($\boldsymbol{\gamma}, \mathbf{s}$) is

$$p(\mathbf{x}_r | \boldsymbol{\gamma}, \mathbf{s}) = \frac{1}{(\pi\sigma^2)^N} \exp\left(-\frac{(\mathbf{x}_r - \mathbf{A}(\boldsymbol{\gamma})\mathbf{s})^H (\mathbf{x}_r - \mathbf{A}(\boldsymbol{\gamma})\mathbf{s})}{\sigma^2}\right) \quad (33)$$

The ML estimation of $\boldsymbol{\gamma}$ and \mathbf{s} can be found by maximising the conditional probability density function of \mathbf{x}_r with respect to $\boldsymbol{\gamma}$ and \mathbf{s} . If \mathbf{s} is modelled as a deterministic unknown vector and $\boldsymbol{\gamma}$ as a deterministic constant vector then the conditional ML will be

$$\hat{\boldsymbol{\gamma}}, \hat{\mathbf{s}} = \arg \max_{\boldsymbol{\gamma}, \mathbf{s}} \{p(\mathbf{x}_r | \boldsymbol{\gamma}, \mathbf{s})\} \quad (34)$$

The above maximisation gives the estimate of $\hat{\boldsymbol{\gamma}}$ and $\hat{\mathbf{s}}$ as:

$$\hat{\mathbf{s}} = (\mathbf{A}^H \mathbf{A})^{-1} \mathbf{A}^H \mathbf{x}_r, \quad (35)$$

$$\hat{\boldsymbol{\gamma}} = \arg \max_{\boldsymbol{\gamma}} \mathbf{x}_r^H \mathbf{A}(\boldsymbol{\gamma}) (\mathbf{A}^H \mathbf{A})^{-1} \mathbf{A}^H \mathbf{x}_r, \quad (36)$$

It is assumed that no prior knowledge is available for DOAs of $\boldsymbol{\gamma} = [\gamma_1, \gamma_2, \dots, \gamma_K]$. The ML method can detect targets in both cases of

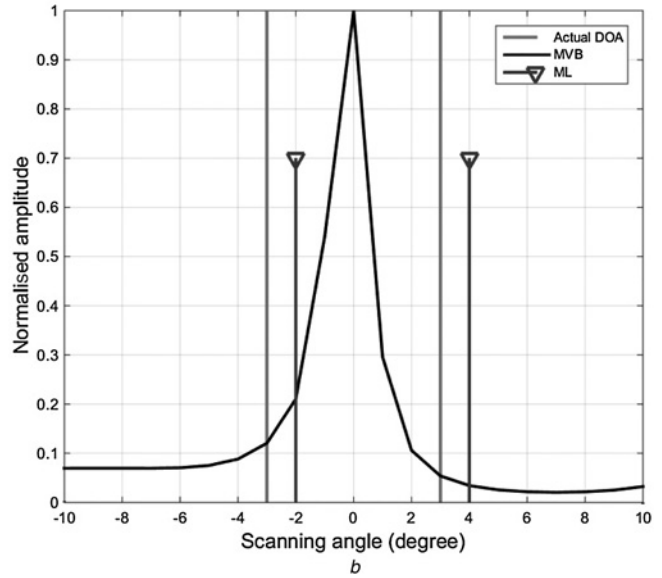
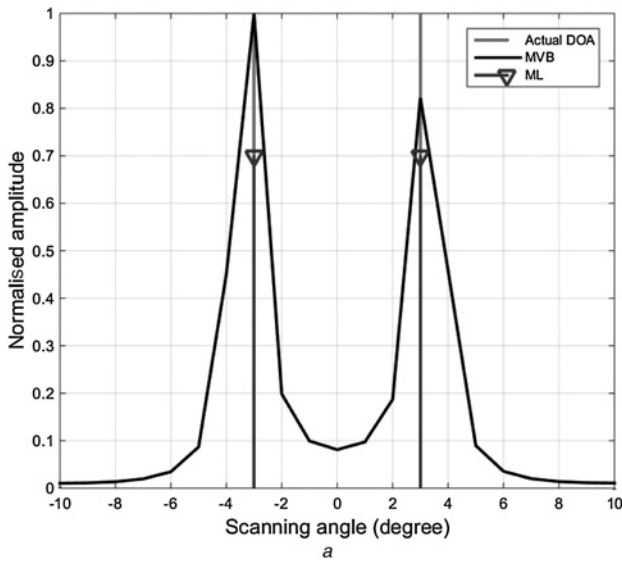


Fig. 3 Results of applying the MVB method along with spatial smoothing and ML method

a SNR = 20 dB
b SNR = 5 dB

correlated and non-correlated signals. It also has good performance in the presence of noise and in the cases where only as few as one scan of the FOV is available. However, for K targets, the ML method requires a K -dimensional search over FOV to find the DOAs. Therefore, when the considered number of targets increases, the ML estimation becomes more computationally intensive. In addition, ML estimation requires prior knowledge of the number of targets. This number has to be estimated in a preprocessing step if no prior information is available.

6 Simulation results

To verify the performance of the proposed methods with respect to different system parameters, a two-way antenna pattern which is approximated using the array factor of a linear array with uniform amplitude weighting as presented in (3) is used.

For this simulation, the carrier frequency is considered to be changing between 8 and 8.5 GHz in $N=21$ steps according to (1). This corresponds to the operation of an FSA described in [24], which scans between -9.7° and 7.7° in non-uniform steps in frequency. The -3 dB beamwidth of these patterns is 13° .

In addition, the Δfov is selected to be the range of $[-6, \dots, 6]^\circ$, and simulations are done to detect targets in this region. As an arbitrary but representative example, a benchmark with two targets is considered. Targets are assumed to be at the same range and at -3° and 3° with respect to boresight. The number of beams in the selected Δfov N and the subvector size Q are selected equal to $N=21$ and $Q_{\text{opt}}=13$ according to (31). The targets amplitude vector s in (14) is assumed to consist of two coherent random complex numbers ($s_2=0.9s_1$) and n is a white Gaussian noise vector. The SNR is defined as the total power of the received signals over the noise power.

Fig. 3 shows the result of applying the MVB method (28) in two different SNR conditions of SNR = 20 and 5 dB. It can be seen that at SNR = 20 dB, the targets are detected at $\gamma_1 = -3^\circ$ and $\gamma_2 = 3^\circ$ (Fig. 3a). However, when SNR = 5 dB the MVB method cannot detect two targets in the Δfov (Fig. 3b). The ML method also detects the targets DOA at $\gamma_1 = -3^\circ$ and $\gamma_2 = 3^\circ$ when SNR = 20 dB and $\gamma_1 = -2^\circ$ and $\gamma_2 = 4^\circ$ when SNR = 5 dB. Note that the interpolation step described in Section 4 is applied with the MVB method. Also note that both methods are implemented with one degree resolution.

To evaluate the performance of the two methods with respect to different parameters, the root mean square error (RMSE) of the targets DOA estimation is calculated. Given the above setup the RMSE is defined as

$$\text{RMSE} = \sqrt{E \left[\sum_{k=1}^K (\gamma_k - \hat{\gamma}_k)^2 \right]}, \quad (37)$$

where $E(\cdot)$ is the expected value estimated using 100 Monte Carlo trials and $K=2$ is the number of targets. The Cramér–Rao Lower Bound (CRLB) [25] which serves as an optimality criterion for DOA estimation is also computed and presented for evaluation of the results. CRLB estimation of real parameters based on a complex data vector with complex Gaussian probability density function is computed according to equations given in [12, 25] with minor modifications and reported in Appendix 1.

Fig. 4 shows the RMSE of DOA estimation obtained with the two methods as a function of the SNR. In that simulation, two targets

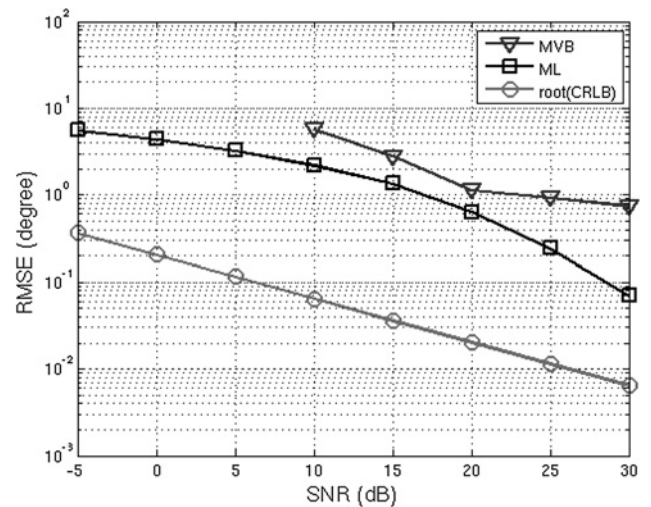


Fig. 4 RMSE of target DOA estimation methods versus SNR for $N=21$, $\gamma_1 = -3$ and $\gamma_2 = 3$

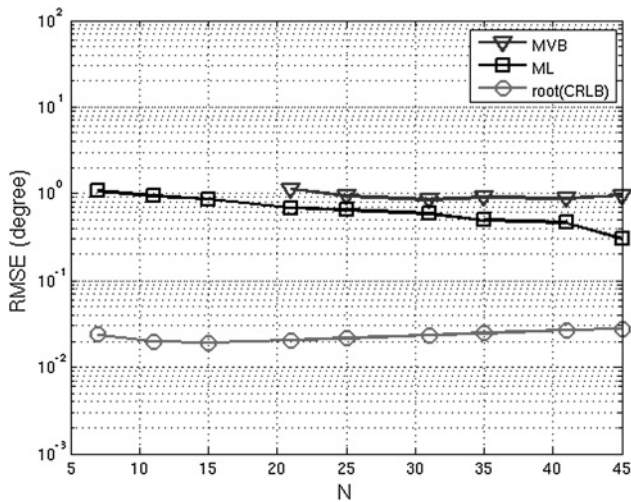


Fig. 5 RMSE of target DOA estimation methods versus N , $SNR = 20$ dB, $\gamma_1 = -3$ and $\gamma_2 = 3$

were also assumed to be at -3° and 3° and the number of beams was also set to $N = 21$. The estimation results in Fig. 4 show that in low SNR situations ($SNR < 10$ dB), the DOA estimation performance is low. For SNR values lower than 10 dB, the ML method can detect two targets with a total error of 4° to 6° and the MVB method cannot detect two targets in the Δfov . For the MVB method, when two targets cannot be separated from each other in more than 5% of the trials, the RMSE values are not plotted in Figs. 4, 5 and 8, as RMSE calculation becomes ambiguous. Also note that both methods are implemented with one degree resolution. Accuracy corresponding to this resolution is achieved when the SNR is above 15 dB for the ML method and above 20 dB for the MVB method.

Fig. 5 shows the RMSE obtained with the two methods as a function of N , the number of beams in the Δfov from the received signal vector. For this simulation, the SNR is fixed at 20 dB and other parameters including the Δfov and the frequency range are kept unchanged. This means that by increasing N , the beams will be closer to each other. It can be seen that for the ML method, increasing N decreases the RMSE. The MVB method also has better performance when the number of beams is large (more than 21). However, this method cannot detect two targets in the Δfov when $N < 21$.

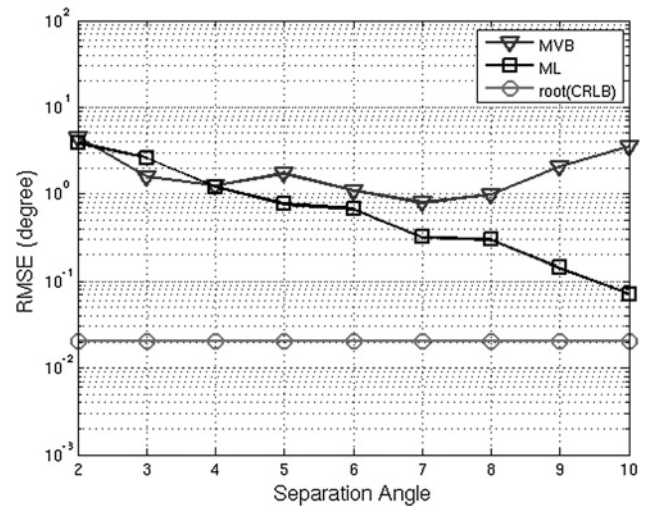


Fig. 6 RMSE of target DOA estimation methods versus angular separation between two targets $SNR = 20$ dB, and $N = 21$

Next, the impact of angular separation of the two targets on the RMSE is studied (Fig. 6). It can be seen that using the ML method, the RMSE decreases when the angular separation between the two targets increases, which means that ML can detect two targets more accurately when they have larger angular distance from each other. However, when using the MVB method, the RMSE increases if the angular separation between two targets is larger than 8° . This is due to the fact that for this simulated antenna patterns and with the current settings, the angular separation between two targets larger than 8° requires sampling from sidelobes of some of the antenna patterns, which decreases the performance of the MVB method.

7 Measured FSA antenna pattern examples

In this section, the performance of the two considered DOA estimation methods is studied by taking into account the antenna patterns of a real FSA antenna. The antenna was designed to work in the X-band and the measured antenna patterns are used in the simulations.

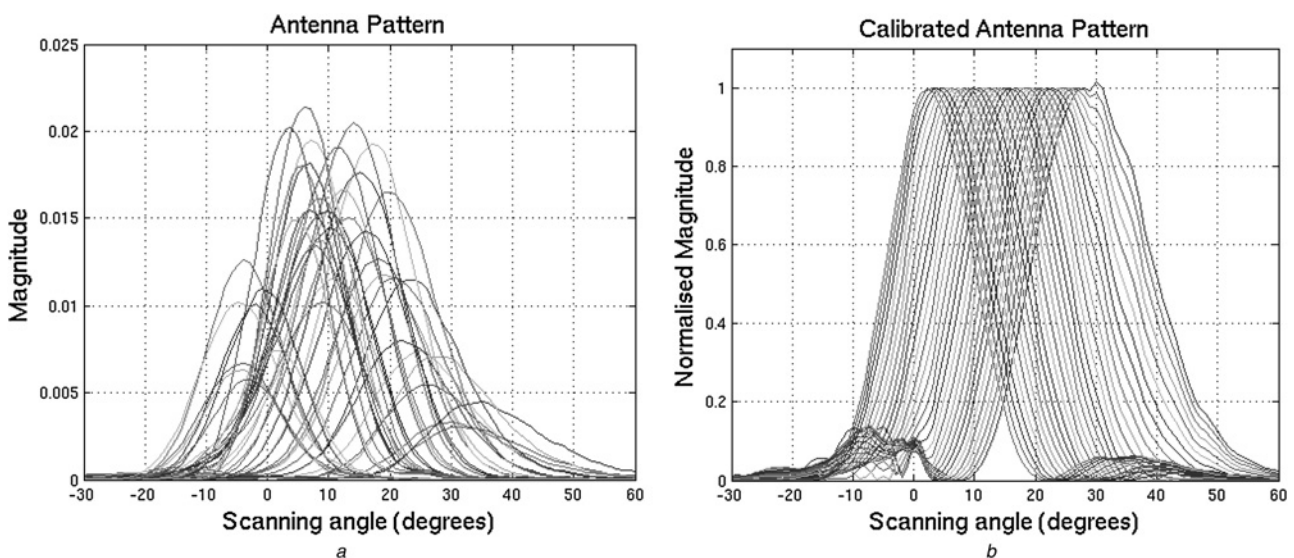


Fig. 7 Measured FSA two-way antenna gain pattern in the range 8–8.8 GHz with frequency steps of 20 MHz

a Non-calibrated
b Calibrated beams for $N = 31$

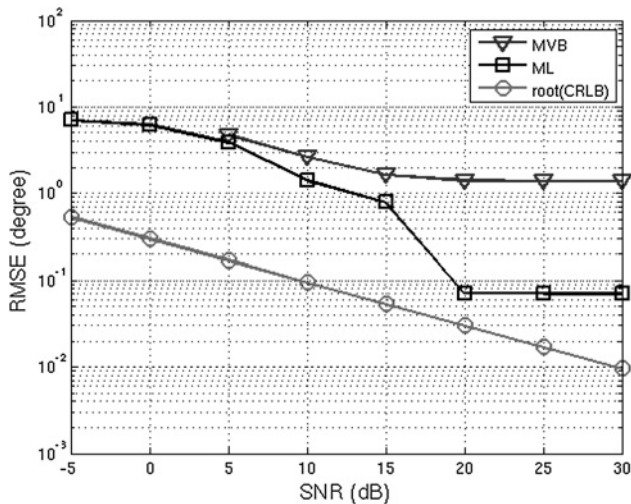


Fig. 8 DOA estimation RMSE versus SNR for $N = 31$, $\gamma_1 = 9^\circ$ and $\gamma_2 = 21^\circ$

Fig. 7a shows the two-way radiation pattern of an 8-element FSA, which is built based on a composite right/left-handed (CRLH) waveguide with air-filled double-ridge waveguide [24]. The antenna scans the angles between -5° and 35° by changing the frequency from 8 to 8.8 GHz in 40 steps. The half-power beamwidth of the antenna varies between 15° and 21° for the different steering angles. This FSA antenna can scan the FOV continuously with controllable frequency steps.

The Δfov is selected to be the range of $[6 \dots 24]^\circ$, and simulations are done to detect targets in this region. As an arbitrary but representative example, a benchmark with two targets is considered. Targets are to be at the same range and at 9° and 21° with respect to boresight. The number of beams in the selected Δfov N and the subvector size Q are selected equal to $N = 31$ and $Q_{\text{opt}} = 19$ according to (31). The targets amplitude vector s in (14) is assumed to consist of two coherent random complex numbers and n is a vector of white Gaussian noise.

In this FSA, the beamwidth and the gain of the antenna main beam is changing for the various steering angles (Fig. 7a). Furthermore, the antenna steering angle changes non-linearly when the frequency is changed in uniform steps. Therefore, the compensation methods discussed in Section 4 is applied before applying the MVB method. Fig. 7b shows the calibrated antenna patterns.

Fig. 8 shows the RMSE of DOA estimation for the two methods as a function of the SNR. The estimation results in Fig. 8 show that in

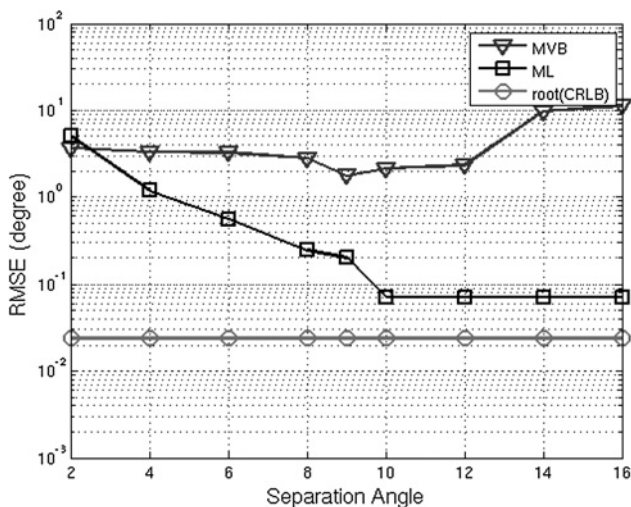


Fig. 9 DOA estimation RMSE versus angular separation between two targets SNR = 20 dB, and $N = 31$

low SNR situations (SNR < 5 dB), the ML method can detect two targets with total error of 4° to 7° while the MVB method cannot separate two targets in more than 5% of trials and therefore is not plotted.

Fig. 9 shows the impact of angular separation of two targets on the RMSE. The achieved results agree with the results in the previous section. It can be seen that using the ML method, the RMSE decreases when the angular separation between two targets increases, which shows that the ML method can detect two targets more accurately when they have more angular distance from each other. However, using the MVB method, the RMSE increases when the angular separation between two targets is larger than 12° . Again, this is due to the fact that for this FSA and with the current settings, the angular separation between two targets larger than 12° requires sampling from sidelobes of antenna patterns, which decreases the performance of the MVB method.

8 Conclusions

In this work, we addressed the problem of resolving the DOA of multiple radar targets separated by less than an antenna beamwidth using FSA antennas. The FSAs are advantageous because frequency scanning can be done very rapidly and accurately, therefore it is easier to track moving targets.

The performance of two DOA estimation algorithms, MVB and ML estimation are studied. These methods were first adapted for our signal model and their performance were investigated through Monte Carlo simulations and compared against each other in terms of RMSE. Simulation results showed that in low SNR situations, the RMSE of DOA estimation is large and the MVB method cannot separate two targets. In addition, it was shown that sampling from sidelobes of the antenna pattern decreases the performance of the MVB method. In other cases, by selecting correct parameters, both methods can separate targets with angular separations smaller than the antenna pattern beamwidth. We have also presented a calibration scheme which worked efficiently when it was applied to different antenna pattern shapes at each frequency and non-uniform scanning angles. In the next step, the proposed methods will be applied to the experimental data captured from a radar experiment using real targets.

9 References

- 1 Yang, N., Caloz, C., Wu, K.: 'Full-space scanning periodic phase-reversal leaky-wave antenna', *IEEE Trans. Microw. Theory Tech.*, 2010, **58**, (10), pp. 2619–2632
- 2 Dong, Y., Itoh, T.: 'Substrate integrated composite right-/left-handed leaky-wave structure for polarization-flexible antenna application', *IEEE Trans. Antennas Propag.*, 2012, **60**, (2), pp. 760–771
- 3 Hansen, R.C.: 'Phased array antennas' (John Wiley & Sons, 2009, 2nd edn.)
- 4 Johnson, D.G.: 'Development of a high resolution MMW radar employing an antenna with combined frequency and mechanical scanning'. IEEE Radar Conf., Italy, Rome, May 2008, pp. 1–5
- 5 Alvarez-Lopez, Y., Garcia-Gonzalez, C., Vazquez-Antuna, C., et al.: 'Frequency scanning based radar system', *Prog. Electromagn. Res.*, 2012, **132**, pp. 275–296
- 6 Alvarez, Y., Cambior, R., Garcia, C., et al.: 'Submillimeter-wave frequency scanning system for imaging applications', *IEEE Trans. Antennas Propag.*, 2013, **61**, (11), pp. 5689–5696
- 7 Stoica, P., Soderstrom, K.: 'Maximum likelihood methods for direction-of-arrival estimation', *IEEE Trans. ASSP*, 1990, **38**, (7), pp. 1132–1143
- 8 Schmidt, R.O.: 'Multiple emitter location and signal parameter estimation', *IEEE Trans. Antennas Propag.*, 1986, **34**, (3), pp. 276–280
- 9 Roy, R., Paulraj, A., Kailath, T.: 'Direction-of-arrival estimation by subspace rotation methods—ESPRIT'. Int. Conf. Acoust. Speech & Signal Processing, April 1986, vol. 11, pp. 2495–2498
- 10 Capon, J.: 'High resolution frequency-wave number spectrum analysis', *Proc. IEEE*, 1969, **57**, (8), pp. 1408–1418
- 11 Liu, G.Q., Yang, K., Sykora, B., et al.: 'Range and azimuth resolution enhancement for 94 GHz real-beam radar', *SPIE 6947 Radar Sens. Technol. XII*, 2008, p. 694701
- 12 Farina, A., Gini, F., Greco, M.: 'DOA estimation by exploiting the amplitude modulation induced by antenna scanning', *IEEE Trans. Aerosp. Electron. Syst.*, 2002, **38**, (4), pp. 1276–1286
- 13 Akhdar, O., Carsenat, D., Decroze, C., et al.: 'A simple technique for angle of arrival measurement'. Proc. IEEE Antennas and Propagation Society Int. Symp., San Diego, USA, July 2008, pp. 1–4

- 14 Akhdar, O., Mouhamadou, M., Carsenat, D., *et al.*: 'A new CLEAN algorithm for angle of arrival denoising', *IEEE Antennas Wirel. Propag. Lett.*, 2009, **8**, pp. 478–481
- 15 Ly, C., Dropkin, H., Manitiuis, A.Z.: 'Array processing application: angular superresolution for scanning antenna'. 33rd Asilomar Conf. on Signals, Systems, and Computers, Pacific Grove, USA, October 1999, pp. 164–168
- 16 Shan, T.J., Wax, M., Kailath, T.: 'On spatial smoothing for direction-of-arrival estimation of coherent signals', *IEEE Trans. ASSP*, 1985, **33**, (4), pp. 806–811
- 17 Uttam, S., Goodman, N.A.: 'Superresolution of coherent sources in real-beam data', *IEEE Trans. Aerosp. Electron. Syst.*, 2010, **46**, (3), pp. 1557–1566
- 18 Farina, A., Gabatel, G., Sanzullo, R.: 'Estimation of target direction by pseudo-monopulse algorithm', *Signal Process.*, 2000, **80**, (2), pp. 295–310
- 19 Gini, F., Bordoni, F., Farina, A.: 'Multiple radar targets detection by exploiting induced amplitude modulation', *IEEE Trans. Signal Process.*, 2004, **52**, (4), pp. 903–913
- 20 Greco, M., Gini, F., Farina, A., *et al.*: 'Direction-of-arrival estimation in radar systems: moving window against approximate maximum likelihood estimator', *IET Radar/Sonar Navig.*, 2009, **3**, (5), pp. 552–557
- 21 Lie, J.P., Blu, T., See, C.M.S.: 'Single antenna power measurements based direction finding', *IEEE Trans. Signal Process.*, 2010, **58**, (11), pp. 5682–5692
- 22 Friedlander, B., Weiss, A.J.: 'Direction finding using spatial smoothing with interpolated arrays', *IEEE Trans. Aerosp. Electron. Syst.*, 1992, **28**, (2), pp. 574–587
- 23 Gershman, A.B., Ermolaev, V.T.: 'Optimal subarray size for spatial smoothing', *IEEE Signal Process. Lett.*, 1995, **2**, (2), pp. 28–30
- 24 Siaka, F.: 'Antenne à balayage de faisceau angulaire avec faible variation de la fréquence'. PhD Thesis, Ecole Polytechnique de Montreal, 2015
- 25 Kay, S.M.: 'Fundamentals of statistical signal processing, volume I: estimation theory' (Prentice-Hall, Englewood Cliffs, NJ, 1993)

10 Appendix

10.1 Appendix 1: CRLB calculation

Considering the complex-value amplitude s being a deterministic unknown vector and defined as $s_i = A_i e^{j\theta_i}$, then the vector of unknown parameters will be $\zeta = [\gamma_1, \dots, \gamma_K, A_1, \dots, A_K, \theta_1, \dots, \theta_K]$.

In addition, assuming that \mathbf{n} is modelled as white complex Gaussian noise with zero mean and covariance matrix of $\sigma^2 \mathbf{I}$,

then the Fisher information matrix [16] for our signal model in (2) can be written as

$$J_{ij} = [\mathbf{J}]_{ij} = \frac{2}{\sigma^2} \operatorname{Re} \left\{ \frac{\partial \boldsymbol{\mu}^H}{\partial \zeta_i} \frac{\partial \boldsymbol{\mu}}{\partial \zeta_j} \right\}, \quad (38)$$

where $\boldsymbol{\mu} = E\{\mathbf{x}_r\} = \sum_{k=1}^K s_k \mathbf{a}(\gamma_k)$. For the first K elements of ζ that represent unknown targets DOA, we have

$$\frac{\partial \boldsymbol{\mu}}{\partial \zeta_i} = s_i \boldsymbol{\vartheta}_i \quad \text{for } 1 \leq i \leq K, \quad (39)$$

where $\boldsymbol{\vartheta}_i$ is the vector with elements of:

$$[\boldsymbol{\vartheta}_i]_n = H_n \frac{N_e \beta d \cos(N_e u) \sin(N_e u) \cos(\gamma_i)}{\sin^2(u)} - \frac{\beta d \cos(u) \sin^2(N_e u) \cos(\gamma_i)}{\sin^3(u)} e^{-j2\pi f_n t_i}, \quad (40)$$

and

$$u = \beta d \left[\sin(\gamma_i) - \sin\left(\theta_1 + \frac{n}{N} (\Delta \text{fov})\right) \right] / 2.$$

The CRLBs are then calculated from diagonal elements of \mathbf{J}^{-1} as $\text{CRLB}(\gamma_i) = [\mathbf{J}]_{ii}^{-1}$. Therefore, for one target ($K=1$), the CRLB (γ_i) will be

$$\text{CRLB}(\gamma_i) = \frac{1}{2\text{SNR}} \operatorname{Re} \{ \boldsymbol{\vartheta}_i^H \boldsymbol{\vartheta}_i \} \quad (41)$$

Copyright of IET Radar, Sonar & Navigation is the property of Institution of Engineering & Technology and its content may not be copied or emailed to multiple sites or posted to a listserv without the copyright holder's express written permission. However, users may print, download, or email articles for individual use.